On the use of power reflection ratio and phase change to determine the geometry of a blockage in a pipe

Wenbo Duan*

Brunel Innovation Centre, Brunel University, Uxbridge, Middlesex, UK, UB8 3PH

Ray Kirby

School of Engineering and Design, Brunel University, Uxbridge, Middlesex, UK, UB8 3PH

Jevgenija Prisutova

Department of Mechanical Engineering, University of Sheffield, Sheffield, UK, S1 3JD

Kirill V. Horoshenkov

Department of Mechanical Engineering, University of Sheffield, Sheffield, UK, S1 3JD

** Corresponding author*

e-mail: Wenbo.Duan@brunel.ac.uk

Key words: guided wave; blockage detection; phase change; inverse technique.

ABSTRACT

Blockages may be detected in pipes by sending acoustic signals down the pipe and measuring the echo from the blockage. This presents a fast and efficient way of determining the presence of a blockage and this method is now being used, for example, to probe the integrity of sewer systems. In this article a method is presented for obtaining both the length and the equivalent cross-sectional area of a blockage using only a single microphone to capture the incident and reflected pulse. The method presented uses the change in phase between the incident and reflected acoustic signals caused by a blockage, as well as the difference in the amplitude of each pulse, to generate two independent equations from which the area ratio and the length of the blockage may be recovered. This requires measurements to be carried out in the plane wave region of the pipe, however it is shown that through appropriate processing of each signal in the frequency domain the area ratio and length of a relatively large number of blockages can be successfully recovered.

1. INTRODUCTION

It is common to use a sound source to probe the conditions of a duct or pipeline. The use of sound is attractive as it provides a non-destructive method for locating items such as defects in pipelines, or in establishing the geometry of a remote section of ductwork. Engineering applications include the monitoring of blockages, cracks and leaks in pipelines [1,2] and the quality control of musical instruments [3]. In each application a remote sound source is used to launch a short pulse, which is then reflected back by the object of interest. A comparison between the properties of the incident and reflected pulse then permits an inverse analysis aimed at finding the geometrical characteristics relating to the test object. It is common

practice here to use a pulse of limited frequency bandwidth and then to directly compare the amplitudes of the incident and reflected pulse [1], or alternatively to deconvolve the measured reflection with the incident pulse and measure the impulse response function of the test object [2-5]. For example, a lossy 'layer peeling algorithm' is often used to reconstruct the area changes of tubular musical wind instruments based on impulse response measurements [2-5]. However, the axial resolution of this algorithm is directly related to the sampling frequency, and the sampling frequency is limited by the radius and length of the pipe because a plane wave assumption is used in the algorithm. Consequently, the layer peeling algorithm cannot be readily applied to sewer system blockage detection applications because the radius and the length of the pipe are both much larger than those used in musical instruments. Accordingly, this article seeks to determine the characteristics of a blockage placed within a pipe by comparing the amplitude and phase of the incident pulse and the pulse reflected by the blockage. This has a number of applications, for example in the investigation of the integrity of gas pipelines [6], or in the location of blockages in sewer systems [7] which is the application of interest in this article.

It is, of course, straightforward to locate a blockage in an acoustic waveguide using time of flight calculations [6], but in order to obtain additional information, such as the size of the blockage some further signal processing is required. For example, Antonopoulos-Domis [8] used a frequency domain technique that measured the axial resonant frequency of the duct with and without the blockage present in order to recover the cross sectional area and the location of the blockage. Qunli and Fricke [9] used a similar method for a duct with a rigid termination, and it was also shown that similar results may be obtained using multiple axial resonant frequencies for closed-closed and closed-open duct geometries [10]. However, those methods that require measurements to be taken with and without a blockage have

limited use in applications where one does not normally have prior access to an empty duct. To address this issue, Qunli [11] later showed that the axial duct eigenfrequency without a blockage can be estimated from measurements taken only with the blockage in place in a pipe with closed-open boundary conditions, although this method is limited to blockages that are asymmetric about the axial midpoint of the duct. By measuring both the resonance and anti-resonance frequencies in a duct de Salis and Oldham [12] showed that it is possible to use a similar technique to recover blockage area for closed-open boundary conditions. This method requires measuring under anti-resonance conditions within the duct so that the acoustic pressure is very small at the closed end of the duct; the authors note that ability to locate the anti-resonance frequencies corresponding to pressure minima is likely to be affected by background noise, and so a deterministic maximum length sequence was used to drive the loudspeaker in order to minimise this problem. It was also later shown by the same authors [13] that by using Qunli's approach [11] one could also remove the requirement to undertake additional measurements for an unblocked duct. Accordingly, techniques are now available that can reconstruct the blockage area in a duct of finite length, provided at least one well defined boundary condition is present such as a rigid or open duct termination. However, a reliance on generating axial resonances within the duct does limit the length of the duct that may be studied successfully.

If one wishes to remove restrictions such as limited duct length and/or the presence of a well-defined duct termination, then it is possible to use a narrow band pulse and to apply techniques such as pulse reflectometry. This method is attractive because it allows for the straightforward separation of the incident and reflected signals and one can easily filter out reflections from say, a termination and/or other known area discontinuities in the duct. Examples of pulse reflectometry applications can be found in the literature, see for example

[1-7], and this method is particularly popular in the reconstruction of the bore size of musical instruments. Sharp and Campbell [2] also show that pulse reflectometry can be used to obtain the complex input impedance of a pipe using its impulse response, which can be used to obtain the depth and radius of a leak. Since the depth of the leak is the same as the thickness of the pipe, Sharp and Campbell proposed a technique to estimate the radius of the hole from the measured input impedance of the pipe.

The lossy 'layer peeling algorithm'[14, 15] is often used in pulse reflectometry applications to reconstruct cross-sectional area change of the pipe as a function of discretised axial coordinates. To do so the impulse response of the test object must be measured first. The area change of the pipe is then calculated using amplitude reflection ratios in a time domain sample by sample basis. This algorithm requires a fine sampling frequency to be used, which limits its application to relatively small and short objects. The layer peeling method also suffers from cumulative errors, especially due to low frequency components, and the 0Hz frequency component in the impulse response measurement can produce a systematic offset to the reconstruction profile. To address these issues, Sharp and Li [16] proposed the insertion of a calibration tube between the source tube and the test object to remove the offset. Furthermore, the impulse response spectrum is improved by combining the low frequency components measured using a bass loudspeaker, with the higher frequency components measured using a compression-driver loudspeaker. Amir et al. [17] later investigated the presence of corrosions, blockages etc. in a condenser pipe using pulse reflectometry. It is shown that the characteristics of the discontinuity can be revealed from the form of the reflected pulse. For instance, a constriction will create a positive reflection, whereas a dilation (increase in cross section) will create a negative reflection. However, the size of the blockage or corrosion is not revealed.

The standard pulse reflectometry normally involves the use of a short transient pulse as the incident signal. Kemp et al. [5] showed that it is possible to use a logarithmic sine sweep signal in such applications, which has the advantage that the energy of the incident signal can be increased. Good signal to noise ratio is achieved using a signal lasting of the order of 10 s. In this case, the forward and backward going waves between the sound source and the test object superimpose. Kemp et al. proposed a multi microphone technique to separate these waves. The system impulse response can then be performed by deconvolving the forward and backward going waves. Kausel [18,19] developed a similar optimisation method to reconstruct the area changes of tubular musical wind instruments based on the frequency domain input impulse response measurement. The input impulse response of the arranged instrument is calculated from a one-dimensional plane wave model, and the optimisation parameters are then changed until the calculated input impulse response match the actual measured input impulse response.

In this paper, an alternative inverse technique is proposed to reconstruct the area ratio and the length of a blockage in a relatively long and large pipe. Standard pulse reflectometry is used, and a short transient pulse is projected into the pipe. The incident and the reflected pulses are separated in the time domain, provided that the distance between the microphone, loudspeaker and the blockage is large enough to avoid signal overlapping. These pulses are then transformed into the frequency domain. The phase change between the incident and reflected pulse is combined with the power reflection ratio to determine the area ratio and the length of the blockage at a single frequency. Multiple frequencies allow an over-determined problem to be formed, and most accurate predictions can be selected at places where signal to noise ratio is high. The inverse technique has a major advantage over previous techniques due

to its simplicity. Unlike the layer peeling algorithm which requires complex signal processing procedures, the method we propose is based on simple analytical expressions which are very easy to implement. This method also avoids the need to measure the impulse response of the blockage, and thus does not suffer from bandwidth limitations or offset problems. However, this method can only give an averaged area ratio and cannot calculate area changes of the blockage in the axial direction. This is not a problem for engineering applications since the relative size of the blockage is of most interest whereas the shape and subtle area changes are not as important. The underlying principle of this technique is discussed in section 2. The method is then implemented in section 3 using experimental measurements taken for 14 different blockages and its success is reviewed in terms of robustness and accuracy in section 4.

2. THEORY

The technique described here is a pulse reflectometry technique that relies on the measurement of an incident and reflected narrow band pulse propagating in a pipe. This requires the study of guided waves, which can be problematic because the sound energy propagates in the form of duct modes. Accordingly, one is always faced with a decision on how many modes, and also which modes, to adopt when undertaking an inverse analysis in a waveguide. For example, in the ultrasonic non-destructive testing of pipelines one normally has no choice but to tolerate the presence of higher order modes and this can add significant difficulties to the interpretation of data reflected from a defect. For an acoustic waveguide it is much more straightforward to restrict the analysis to the propagation of a single, planar mode, simply by careful choice of the centre frequency of the incident pulse; however, this

has the potential disadvantage of limiting the amount of information one may obtain for the blockage. Therefore, one must balance the amount of information required about the blockage with the difficulty in processing the modal-based information scattered by the blockage. In this article, analysis is restricted to the plane wave region only and it will be shown that this is sufficient to recover the area ratio and the length of the blockage. Whilst it is attractive to make use of higher order modes, maybe to try and recover more information about the shape of the blockage, this has been found to be very difficult to do, even under very controlled laboratory conditions [20]. This is believed to be because higher order modes are very sensitive to the boundary conditions in a duct and this sensitivity makes it difficult to develop a reliable and robust technique suitable for use under less controlled conditions, such as sewer systems [20]. Furthermore, higher order modes are dispersive and so this makes a methodology that utilises a change in phase more difficult to implement. Accordingly, the emphasis of this article is on developing an approach for use in industrial applications that is both reliable and robust.

For plane wave propagation a simple set of analytic expressions may be obtained provided one matches continuity of pressure and volume velocity over the area discontinuities at each end of the blockage, see planes 1 and 2 in Fig. 1. This is, of course, an approximation of the true matching conditions and so errors will be apparent even for the plane wave region. Therefore, in order to investigate the effect of these errors, the plane wave based predictions will be compared against a full treatment of the problem (based on a mode matching approach) in section 3 [20, 21].

For plane wave propagation, one may write the sound pressure as a sum of the incident and reflected plane waves propagating in any particular region; thus, for region q,

$$p_q(x) = A_q e^{-ikx} + B_q e^{ikx}, \tag{1}$$

and the velocity is given as

$$\rho c u_q(x) = A_q e^{-ikx} - B_q e^{ikx}, \tag{2}$$

where a time dependence of $e^{i\omega t}$ is assumed with t denoting time, ω the radian frequency and $i = \sqrt{-1}$. In addition ρ is the fluid density, c is the speed of sound, p is pressure, u is the particle velocity, A_q and B_q are the amplitudes of the incident and reflected waves in the region q, and $k = \omega/c$ is the wavenumber in air. The origin of the x coordinate is defined on plane 1.

For waves propagating in region 1 the sound pressure and volume velocity on plane 1 is $A_1 + B_1$ and $S_1(A_1 - B_1)/\rho c$, respectively, where S_q denotes pipe cross-sectional area in region q. For waves propagating in region 2, there will be a phase delay between the sound pressure and velocity on planes 1 and 2, and the sound pressure and volume velocity on plane 1 is $A_2 + B_2$ and $S_2(A_2 - B_2)/\rho c$, respectively. The sound pressure and volume velocity on plane 2 is $A_2 e^{-ikL_b} + B_2 e^{ikL_b}$ and $S_2\left(A_2 e^{-ikL_b} - B_2 e^{ikL_b}\right)/\rho c$, respectively, where L_b is the length of the blockage.

For waves propagating in region 3, the sound pressure and volume velocity on plane 2 is $A_3 e^{-ikL_b}$ and $S_3 A_3 e^{-ikL_b}/\rho c$, respectively. To simplify the development of the equations that follow the modal amplitude in region 3 is normalised so that $A_3 = A_3' e^{ikL_b}$. Furthermore, regions 1 and 3 have identical cross-sectional areas so that $S_1 = S_3$. Here it has also been assumed that there is no reflection from the far end of region 3. This means that in the experimental measurements the width of the incident pulse in the time domain must be sufficiently small so that any signal reflected by the end of the pipe (or other obstructions in a real sewer system) do not interact with the transmitted signal. This is relatively easy to achieve under laboratory conditions, and it is also common to adopt such practice in field tests.

Matching pressure and volume velocity over planes 1 and 2, thus delivers the following equations:

$$A_1 + B_1 = A_2 + B_2 \tag{3}$$

$$A_1 - B_1 = [A_2 - B_2]/\sigma \tag{4}$$

$$A_2 e^{-ikL_b} + B_2 e^{ikL_b} = A_3' \tag{5}$$

$$A_2 e^{-ikL_b} - B_2 e^{ikL_b} = \sigma A_3' \tag{6}$$

Here, σ is the area ratio, defined as $\sigma = S_1/S_2$. It is straightforward to eliminate A_2 and B_2 from Eqs. (3) to (6) and to write

$$A_1 = \frac{A_3'}{2\sigma}[2\sigma \cos kL_b + (\sigma^2 + 1) i \sin kL_b] \tag{7}$$

and

$$B_1 = \frac{A_3'}{2\sigma}(\sigma^2 - 1)i\sin kL_b \tag{8}$$

It is convenient now to work with the sound power, so that the power reflection ratio Λ is defined as

$$\Lambda = \frac{|B_1|^2}{|A_1|^2}, \tag{9}$$

and the tangent of the phase difference ψ on plane 1 is defined as

$$\psi = \frac{\mathrm{Im}(B_1/A_1)}{\mathrm{Re}(B_1/A_1)}. \tag{10}$$

Substitution of Eqs. (7) and (8) into Eqs. (9) and (10) yields

$$\Lambda = \frac{(\sigma^2 - 1)^2}{(\sigma^2 + 1)^2 + 4\sigma^2 \cot^2 kL_b}, \tag{11}$$

and

$$\psi = \frac{2\sigma \cot kL_b}{\sigma^2 + 1}. \tag{12}$$

The task now is to re-write Eqs. (11) and (12) so that one may solve separately for the length and area ratio of the blockage. For the area ratio this delivers a quadratic equation, which has the general solution

$$\sigma^2 = \frac{\Lambda(1+\psi^2)+1 \pm 2\sqrt{\Lambda(1+\psi^2)}}{1-\Lambda(1+\psi^2)}. \tag{13}$$

Note here that the two solutions for σ^2 simply deliver values for S_1/S_2 and S_2/S_1, this is because for the plane wave region the governing equations of an area expansion and area reduction are identical. Finally, for the blockage length,

$$L_b = \frac{1}{k}\cot^{-1}\left[\frac{(\sigma^2+1)\psi}{2\sigma}\right] + \frac{n\pi}{k}, \qquad n = 0,1,2,.... \tag{14}$$

Here, there are an infinite possible number of solutions for L_b at each frequency. However it will be shown in the next section that the length can readily be recovered provided that σ and L_b can be obtained from a number of different frequencies, which permits the subsequent averaging of data in order to deliver more reliable predictions. Furthermore, in Eqs. (3) and (4) the origin of the x coordinate is defined at plane 1 and so e^{-ikx} and e^{ikx} terms in Eqs. (1) and (2) disappear. However, the microphone is not placed at plane 1, this means that one must account for the attenuation and phase shift introduced by the pipe as the pulse propagates from the microphone to the blockage (plane 1) and back again. This effect is discussed further in the next section.

3. EXPERIMENT

The experimental apparatus consists of a blockage of arbitrary shape placed inside a cylindrical PVC pipe with an internal diameter of 150 mm. At one end of the pipe is a Fané compression driver, which is placed against the end wall of the pipe to simulate a point

source. The blockage is placed at a distance of $L_1 = 12$ m from the sound source, and the distance from the end of the blockage to the far (open) end of the pipe is $L_2 = 6$ m. A Knowles Acoustics MEMS microphone is placed at a distance of $L_1 - L_\mathrm{m} = 6$ m away from the sound source. Experimental measurements are taken at room temperature so that the speed of sound $c = 343.2$ m/s, and density $\rho = 1.225$ kg/m^3. A Gaussian weighted sinusoidal signal

$$f(t) = a_0 \sin(\omega t)\, e^{-(t-\mu)^2/\tau^2}, t \geq 0 \tag{15}$$

is emitted by the driver. Here, μ is the position of the centre of the pulse, and τ controls the width of the pulse. For the experiments undertaken here $\mu = 2T$, $\tau = T$ and $T = 1/f_0$, where f_0 is the centre frequency of the pulse. A National Instruments DAQ NI PXIE-6358 system was used to acquire the signal from the microphone. This was controlled using LABVIEW software with a sampling rate of 48 kHz. Measurements were undertaken in the plane wave region of the pipe and carried out at five centre frequencies of 200, 400, 600, 800 and 1000 Hz. Five pulses were used to ensure that each pulse has a modest signal width in the time domain. For each measurement, the incident and reflected pulse are truncated and then Fourier transformed into the frequency domain. The distances between the microphone position, blockage and pipe end are sufficiently long to avoid signal overlap. In order to increase the signal to noise ratio, measurements are also obtained only for a relatively narrow frequency bandwidth so that for a centre frequency f_0 data are taken from $(f_0 - 100)$ Hz to $(f_0 + 80)$ Hz, which corresponds to a maximum sound power drop of 20dB. The use of five different centre frequencies permits a frequency range from 100Hz to 1080Hz to be covered. It should be noted that the choice of frequencies depends on the radius of the pipe, so that the upper frequency limit should fall well below the frequency at which the first high-order mode

cuts on. For the pipe studied here this frequency is 1340Hz [22] and so the measurements were limited to an upper centre frequency of 1080Hz. A further benefit of using multiple pulses is that the reflection characteristics of the object being studied are normally frequency dependent. At certain frequencies very little energy will be reflected back and so the use of multiple pulses allows a centre frequency to be chosen where the reflected energy from the blockage is close to maximum.

Before substituting the measured modal power reflection ratios and phase changes into Eqs. (13) and (14), it is necessary first to compensate for the attenuation and phase shift in a pulse when it travels between the observation location and plane 1. To do this the distance from the blockage to the microphone (L_m) is first obtained by measuring the time of flight between the two locations using the incident and reflected pulse. The most obvious way to do this is to measure from the same point at the start of the incident and reflected pulse when viewed in the time domain. However, the start of each pulse is often buried in noise and so measurement error can easily be introduced. This error (x_e) does not affect the amplitude of the attenuation calculations, but will shift the phase by e^{-2ikx_e}. Accordingly, the time of flight is measured here by taking the cross-correlation between the incident pulse and the reflected pulse and measuring the time of flight using the point of maximum cross-correlation. It is observed that the time of flight differs slightly when the pulse frequency is altered. This is because the interaction between each pulse and the blockage changes with a change in centre frequency and so the shape of the reflected pulse changes. Furthermore, the thermal viscous losses are frequency dependent as the pulse propagates along the pipe and the signal is slightly dispersive. Consequently different frequencies will experience slightly different time of flights. To accommodate these variations the time of flight is averaged using the

reflected pulses that have the highest signal to noise ratio. This will also help to maintain the same phase shift error e^{-2ikx_e} because the same x_e is used throughout. Here, the number of pulses used to average the time of flight is determined by the length of the blockage because the number of power reflection ratio peaks in a certain frequency range is directly associated with the length of the blockage.

In this section pipe attenuation is accommodated by factoring attenuation into the experimental measurements by replacing the wavenumber with a factor β, where [22]

$$\beta = k\left[1 + (1-i)\frac{[1+(\gamma-1)\xi]}{Q_n\sqrt{2}}\right] \tag{16}$$

Here, $Q_n = a(\omega/\nu)^{0.5}$, where a is the radius of the pipe, ν is the kinematic viscosity of the air, γ is the ratio of the specific heats and $\xi = 1/\sqrt{P_r}$, with P_r the Prandtl number for the air. This attenuation factor is only used for the wave propagation between the observation location and the blockage. For the incident pulse, a compensation factor of $e^{-i\beta L_m}$ should be used, while a factor of $e^{i\beta L_m}$ should be used for the reflected pulse. The maximum loss in the blockage chamber region (see region 2 in Fig. 1) is less than 0.4% for a 300 mm long blockage up to 1080 Hz, and is negligible compared to the losses between the microphone and the blockage. The losses in region 2 of the pipe are therefore neglected.

It is interesting first to review a comparison between the measured and predicted power reflection ratio Λ and tangent of the phase difference ψ. For this purpose, a uniform axisymmetric blockage is placed in the centre of the pipe. This blockage is a hollow PVC cylinder, tightly covered with wooden lids from both ends. It has a length of $L_b = 305$ mm

and a diameter of 110 mm. In Fig. 2 values for Λ and ψ are presented for five pulses with the centre frequencies described above. The frequencies are normalised in the form of Helmholtz number kd, where d is the diameter of the pipe, and thus the first high order mode in a cylindrical pipe always cuts on at $kd = 3.68$. A kd range of 0-3 will ensure that pulses are reasonably far away from the cut-on frequency, and evanescent modes shall play a less important role. In the plane wave model, Λ and ψ are calculated using Eqs. (11) and (12). It can be seen in Fig. 2(a) that the plane wave model slightly overpredicts the measured power reflection ratio in the frequency range of $kd < 1.5$ and that its spectrum is slightly shifted towards the higher frequency end. The reason for this discrepancy is the approximation inherent in the volume velocity matching conditions used for the inlet and outlet plane of the blockage in the plane wave model. This is confirmed by comparing plane wave predictions with a full finite element model [20,21], which is also shown in Fig. 2. Clearly, the area ratio spectrum predicted by the finite element model is in better agreement with the measured data, although it is seen in Fig. 2(a) that the measured reflection ratio is lower than that predicted by the FEM. Equation (11) shows that when $kL_b = m\pi/2$, $m = 1, 3, 5, ...$, the power reflection ratio Λ will be maximum. In these situations, the length of the blockage is equal to odd integer multiples of a quarter of the wavelength. The first peak $kd = 0.70$ indicates that $kL_b = \pi/2$, and L_b is thus calculated to be 336.6mm. This is larger than the actual blockage length 305mm. The reason is that the actual maximum reflection ratio Λ happens at a frequency slightly lower than the predicted maximum reflection ratio Λ in the plane wave model, which is shown in Fig. 2(a). The second peak $kd = 2.17$ corresponds to $m = 3$. As the frequency increases, the difference between the plane wave model and the FE model increases because evanescent modes are not considered in the plane wave model and these become more influential as one approaches the cut on frequency of the first cross-sectional mode. This discrepancy between a plane wave and FE model in terms of power reflection

ratio was also observed by Kirby [21]. Fig. 2(a) also shows that the maximum difference between the plane wave model and experiment is less than 8% in the frequency range studied here.

In Fig. 2(b) the measured tangent of the phase difference generally agrees well with the predicted value, except near $kd = 1.47$ and 2.94. Around these values the sound power of the reflected signal is almost close to zero, and this makes it difficult to measure the reflected signal accurately. Fig. 2(b) also shows that around $kd = 1.47$ and 2.94, the phase difference between the incident and the reflected wave is around 90^o, so that the tangent of the phase difference is close to infinity (positive or negative). It is clear then that predictions should avoid values close to $kd = 1.47$ or 2.94 where the length of the blockage is equal to integer multiples of a half of the wavelength.

In Fig. 3 the predicted blockage area ratio and length is shown following the application of Eqs. (13) and (14). In view of the results presented in Fig. 2 it is perhaps not surprising to see that the accuracy of this method depends on the centre frequency of the pulse. For example, at frequencies where the maximum sound power is reflected by the blockage, the method is seen to work well, but when little sound power is reflected from the blockage the method is less effective. This is especially true in the prediction of area ratio, where significant problems are observed as the amount of reflected sound power is reduced. In Fig. 3b the length of the blockage is obtained using $n = 0$ and $n = 1$ in Eq. (14), and here reasonably accurate predictions can be obtained. Eqs. (11) and (12) show that the power reflection ratio and tangent of the phase change would remain the same if the length of the blockage is increased by multiples of the half of the wavelength, and this is why infinite solutions are available for the blockage length as shown in Eq. (14). However, in the low frequency range

when $kd < 0.9$ the wavelength is larger than 1 m, and so $n = 0$ and $n = 1$ in Eq. (14) is enough to cover blockages that are less than 1 m long. For the 305 mm blockage used in Figs. 2 and 3, the length of the blockage equals to half of the wavelength around $kd = 1.5$, and so in Fig. 3(b) $n = 0$ corresponds to the true solution when $kd < 1.5$ and $n = 1$ corresponds to the true solution when $kd > 1.5$. Thus, the choice of n is dictated by the wavelength of sound in relation to the length of the blockage.

It is also evident in Fig. 3 that the regions where the reflected signals are strongest are where the calculation of area ratio and length is most successful. Thus, it can be concluded that the relationships obtained in Eqs. (13) and (14) are capable of delivering accurate predictions for the area ratio and length of the blockage, but this relies on a strong incident signal and on good agreement between the predicted and measured power reflection ratios. Thus, the use of five pulses with different centre frequencies is sensible for the success of the current method. This is because these pulses cover a large frequency range that permits the largest reflected sound power to be measured for a particular blockage. The most accurate predictions are then found to be at frequencies where the reflection from the blockage is strongest. For example, in Fig. 2, the reflected sound power is strongest at $kd = 0.70$ and $kd = 2.17$. Five samples of blockage area ratio and length centred at $kd = 0.70$ and $kd = 2.17$ are then averaged to find the blockage geometry. In Fig. 2 this gives a prediction for the area ratio of $\sigma = 0.536$, and a length of $L_b = 0.292$ m, which gives an error of 0.3% for the area ratio, and 4% for the length of the blockage respectively.

Since the inverse model is used in the plane wave region, the technique can be applied to different situations where the blockage is neither axisymmetric nor at the centre of the duct. A series of additional experiments were carried out for different types of blockages and

predictions are compared here with actual blockage sizes. Fig. 4 shows the measured power reflection ratio and predicted blockage area ratio and length for a rectangular brick placed in the pipe. The brick has an area ratio of 0.379 and a length of 218 mm, and is placed at the bottom of the pipe. Following the strategy for predicting the geometry of the blockage outlined above the maximum reflection is measured at $kd = 1.16$ and $kd = 2.89$. These values are larger than those values seen in Fig. 3 and this is because the length of the brick is shorter than the length of the blockage in Fig. 3. Note that when the length of the blockage is less than 200 mm then only the one peak appears in the response for $kd \leq 3$. Furthermore, if the length of the blockage is less than 80 mm, then no peaks are observed and so this represents a limit below which problems of accuracy will be observed with this method. In Fig. 4 five samples of blockage area ratio and length are taken and these are centred at $kd = 1.16$, and three samples are also taken at Helmholtz numbers to the left of $kd = 2.89$. Here, the area of the brick is much less than the area of the blockage used in Fig. 3, however accurate predictions can still be obtained. Thus, the area ratio is predicted here to be 0.382 with an error of 0.8%, and the length of this blockage is predicted to be 204 mm with an error of 6.4%. This represents good agreement between the predicted and actual blockage geometry, even for a relatively complex blockage.

Fig. 5 shows the measured power reflection ratio, the predicted blockage area ratio, and the predicted length for a moulded blockage, which is designed to fit curvature of the pipe. The blockage area ratio is 0.175 and its length is 100 mm. Fig. 5(a) shows that the maximum reflected sound power is less than 5% of the incident sound power. This is because the area of the blockage is small and the majority of the sound power bypasses this blockage. This places a difficulty in measuring the reflection ratio and phase difference accurately, since the reflected signal is very weak. Accordingly, it can be seen in Fig. 5(a) that the agreement

between measurement and prediction is less successful when compared to Figs. 3(a) and 4(a). Here the predicted area ratio is $\sigma = 0.190$ and the predicted length is $L_b = 0.113$ m. This gives an error for the area ratio of 8%, and for the length the error is 13%. This is because the blockage is relatively short when compared to the wavelengths of sound used to excite the object. It is of no surprise here to see that inaccuracies in the measurement of length will appear when the size of the blockage is small when compared to the diameter of the duct, because high resolutions are very difficult to obtain with wavelengths that are long when compared to the geometry of the blockage, and one cannot compensate for this by significantly increasing the frequency of excitation because this will excite higher order modes in the pipe. Thus, the accuracy of this method is limited for relatively short objects in large diameter pipes, although this restriction is likely also to apply to those other methods discussed in the introduction.

In Fig. 6 the measured power reflection ratio, and predicted blockage area ratio and length, are shown for a cylindrical wooden blockage. This blockage has an area ratio of 0.226 and a length of 90 mm, and it is placed at the bottom of the pipe. The length of the blockage is very close to the one used in Fig. 5, and so the reflection ratio has a similar oscillation pattern. The maximum reflection from the blockage is measured to be at $kd = 1.73$ and this yields a predicted area ratio of $\sigma = 0.237$, and a predicted length of $L_b = 0.113$ m; this gives an error of 4.9% for the area ratio and 25.6% for the length. Thus, it can be seen here that the method is generally successful in capturing the geometry of an object that is large enough to deliver sufficient power reflection for a given frequency range, although some errors are inevitable for relatively small objects.

Since the power reflection ratio and the accuracy of the predictions are strongly frequency dependent, a strategy for looking for the blockage area ratio and length can be summarised from the above figures. First, the power reflection ratio curve is obtained from the measured signals containing either one peak (Figs. 5 and 6) or two peaks (Figs. 3 and 4). Second, five frequencies are selected around each maximum in the reflection curve, and five samples of area ratio and length are taken at these frequencies, or three frequencies to the left of the maximum if the maximum frequency is 1080Hz which coincides with the maximum frequency that is being measured. The blockage area ratio and length are then calculated for each frequency taken near the maximum reflection using Eqs. (13) and (14), and an average of these values is then taken to arrive at the final value.

Following the strategy above, a series of further tests were conducted using ten additional blockages and these are summarised in Table 1. Here a range of different blockage geometries are studied in order to investigate the proposed method. The cross-sectional shapes of the blockages are given in Fig. 7. The length L_b in Table 1 is the length of the blockage in the axial direction, and W, H and R are the width, height or radius of the corresponding blockage shown in Fig. 7. Here, all the blockages have been placed at the bottom of the pipe with the cross-section of the blockage perpendicular to the axis of the pipe. It can be seen in Table 1 that most of the blockage area ratio predictions are reasonably accurate, with an error that is generally less than 20% for both the area ratio and the blockage length. The only exception is blockage No. 6 in which an error of 70.6% is observed for the area ratio. The reason for this is that blockage 6 is a small blockage with an area ratio of only 5% and a maximum power reflection ratio of around 1%. Since the reflected signal is so weak, it proved very difficult to obtain a good prediction for this object and so this demonstrates the limit of the present technique in terms of its ability to estimate the area

ratio. However, for the other blockages in Figs. 3 to 6 and in Table 1, the results presented demonstrate that this method is generally successful at recovering the area ratio and length of the blockage. Whilst higher levels of accuracy than those seen here would, of course, be desirable one must also remember that this data has been obtained using only one microphone. Accordingly, one cannot expect very high levels of accuracy over a wide range of different geometries. Moreover, for most applications in which one is interrogating blockages in a waveguide this level of accuracy is generally acceptable. Thus, it is concluded here that this method provides a useful way of determining information about the geometry of a blockage using the phase information contained within a pulse, as well as the more usual amplitude information.

4. CONCLUSIONS

This article investigates a pulse-echo methodology for obtaining the geometry of a blockage in a pipe using only one microphone. The power reflection ratio and phase change of the reflected signal with respect to the incident signal is combined in order to retrieve the characteristics of a blockage. The use of transient pulse signals allows each pulse to be windowed to filter out reflections from each end of the pipe. This method is therefore easier to implement when compared to those methods that use resonance or anti-resonance sound fields where boundary conditions must be carefully controlled. This method is also easier to implement than the layer peeling algorithm which requires complex signal processing procedures.

The performance of this method in the presence of blockages of various shapes and dimensions has been investigated using pulses with different centre frequencies. These frequencies have been chosen to ensure plane wave propagation in the pipe and to permit the

measurement of the frequency response of a blockage within a reasonably broad frequency range. Predictions for the area ratio of a blockage are generally seen to be good, with errors of less than 20% for most blockages with a cross-sectional area of greater than 5% of the pipe cross-section. It is also shown that good predictions can be made even when the reflected sound power is around 5% of the incident sound power. For the blockage length, predictions are generally within 30% of the actual value, although problems were observed for relatively short blockages and here it is observed that problems will occur for values of L_b/λ that are less than approximately 0.3 (where λ is the shortest wavelength to be investigated and is a function of the pipe radius).

Accordingly, the results presented here demonstrate that it is possible to recover both the area ratio and the length of a blockage using only one microphone. Moreover, this can be accomplished in a pipe in which no special arrangement has been made regarding the boundary conditions, such as those terminating conditions required by a number of other methods. This means that the method can be used in practical applications, such as sewer pipes, drainage systems and drained clean water pipes. Furthermore, it appears possible to extend this technique to the study of multiple blockages, where the relationship between the incident and transmitted waves associated with each blockage may be obtained through the same equations as those presented here, with the area ratio and length of each blockage being recovered sequentially.

ACKNOWLEDGEMENTS

The authors would like to thank the UK Engineering and Physical Sciences Research Council (Grant numbers EP/H015280/1, EP/H015469 and EP/I029346/1) for their support of the work reported in this article. The authors are grateful to the technical staff at the University of Bradford, and in particular, Mr. Nigel Smith, for support in building the experimental rig.

REFERENCES

1. E.S. Morgan, P.A.E. Crosse, The acoustic ranger, a new instrument for tube and pipe inspection, NDT Int. 11(1978) 179-183.
2. D.B. Sharp, D.M. Campbell, Leak detection in pipes using acoustic pulse reflectometry, Acta Acust. United. Ac. 83(1997) 560-566.
3. J.M. Buick, J. Kemp, D.B. Sharp, M. van Walstijn, D.M. Campbell, R.A. Smith, Distinguishing between similar tubular objects using pulse reflectometry: a study of trumpet and cornet leadpipes, Meas. Sci. Technol. 13(2002) 750-757.
4. A. Li, D.B. Sharp, B.J. Forbes, Increasing the axial resolution of bore profile measurements made using acoustic pulse reflectometry, Meas. Sci. Technol. 16(2005) 2011-2019.
5. J.A. Kemp, M, van Walstijn, D.M. Campbell, J.P. Chick, R.A. Smith, Time domain wave separation using multiple microphones, J. Acoust. Soc. Am. 128(2010) 195-205.
6. K.A. Papadopoulou, M.N. Shamout, B. Lennox, D. Mackay, A.R. Taylor, J.T. Turner, X. Wang, An evaluation of acoustic reflectometry for leakage and blockage detection, P. I. Mech. Eng. C-J. Mec. 222(2008) 959-966.
7. K. Horoshenkov, Acoustical monitoring of water infrastructure, Acoustics 2012, Nantes, France.
8. M. Antonopoulos-Domis, Frequency dependence of acoustic resonances on blockage position in a fast reactor subassembly wrapper, J. Sound Vib. 72(1980) 443-450.
9. W. Qunli, F. Fricke, Estimation of blockage dimensions in a duct using measured eigenfrequency shifts, J. Sound Vib. 133(1989) 289-301.
10. W. Qunli, F. Fricke, Determination of blocking locations and cross-sectional area in a duct by eigenfrequency shifts, J. Acoust. Soc. Am. 87(1990) 67-75.

11. W. Qunli, Reconstruction of blockage in a duct from single spectrum, Appl. Acoust. 41(1994) 229-236.
12. M.H.F. De Salis, D.J. Oldham, Determination of the blockage area function of a finite duct from a single pressure response measurement, J. Sound Vib. 221(1999) 180-186.
13. M.H.F. De Salis, D.J. Oldham, The development of a rapid single spectrum method for determining the blockage characteristics of a finite length duct, J. Sound Vib. 243(2001) 625-640.
14. N. Amir, U. Shimony, G. Rosenhouse, A discrete model for tubular acoustic systems with varying cross section - the direct and inverse problems. Part 1: Theory, Acta Acust. United. Ac. 81(1995) 450-462.
15. N. Amir, U. Shimony, G. Rosenhouse, A discrete model for tubular acoustic systems with varying cross-section - the direct and inverse problems. Part 2: Experiments, Acta Acust. United. Ac. 81(1995) 463-474.
16. D.B. Sharp, A. Li, The problem of offset in acoustic pulse reflectometry, Proceedings of International Symposium on Musical Acoustics 2007, Barcelona, Spain.
17. N. Amir, O. Barzelay, A. Yefet, and T. Pechter, Condenser tube examination using acoustic pulse reflectometry, J. Eng. Gas Turb. Power. 132(2010) 014501_1-5.
18. W. Kausel, Optimization of brasswind instruments and its application in bore reconstruction, J. New Music Res. 30(2001) 69–82.
19. W. Kausel, Bore reconstruction of tubular ducts from its acoustic input impedance curve, IEEE Trans. Instrum. Meas. 53(2004) 1097-1105
20. W. Duan, R. Kirby, J. Prisutova , K. Horoshenkov, Measurement of complex acoustic intensity in an acoustic waveguide, J. Acoust. Soc. Am. 134 (2013) 3674-3685.
21. R. Kirby, Modeling sound propagation in acoustic waveguides using a hybrid numerical method, J. Acoust. Soc. Am. 124(2008) 1930-1940.

22. M. J. Crocker, Handbook of acoustics, John Wiley, New York 1998.

FIGURE CAPTIONS

Fig. 1 Experimental apparatus.

Fig. 2(a) Power reflection ratio Λ , (b) tangent of the phase difference ψ: ——, FE model; ー ー ー , plane wave model; ■ ■ ■ , experiment.

Fig. 3(a) Blockage area ratio, (b) blockage length: ——, FE model; ■ ■ ■ , experiment; ー ー ー , actual blockage size.

Fig. 4(a) Power reflection ratio Λ , (b) blockage area ratio, (c) blockage length: ——, plane wave model; ■ ■ ■ , experiment; ー ー ー , actual blockage size.

Fig. 5(a) Power reflection ratio Λ , (b) blockage area ratio, (c) blockage length: ——, plane wave model; ■ ■ ■ , experiment; ー ー ー , actual blockage size.

Fig. 6(a) Power reflection ratio Λ , (b) blockage area ratio, (c) blockage length: ——, plane wave model; ■ ■ ■ , experiment; ー ー ー , actual blockage size.

Fig. 7 General shapes of the blockages used in Table. 1.

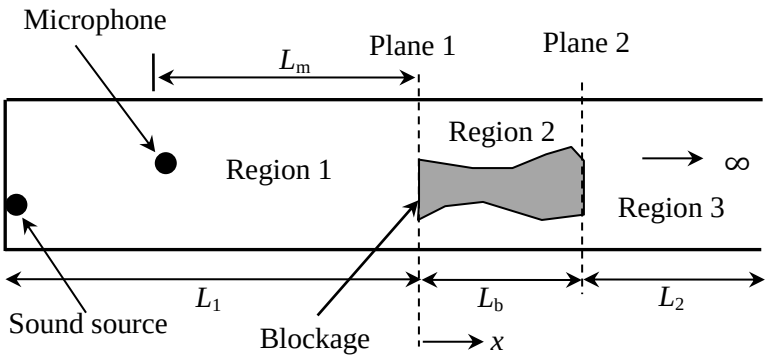

Fig. 1 Experimental apparatus.

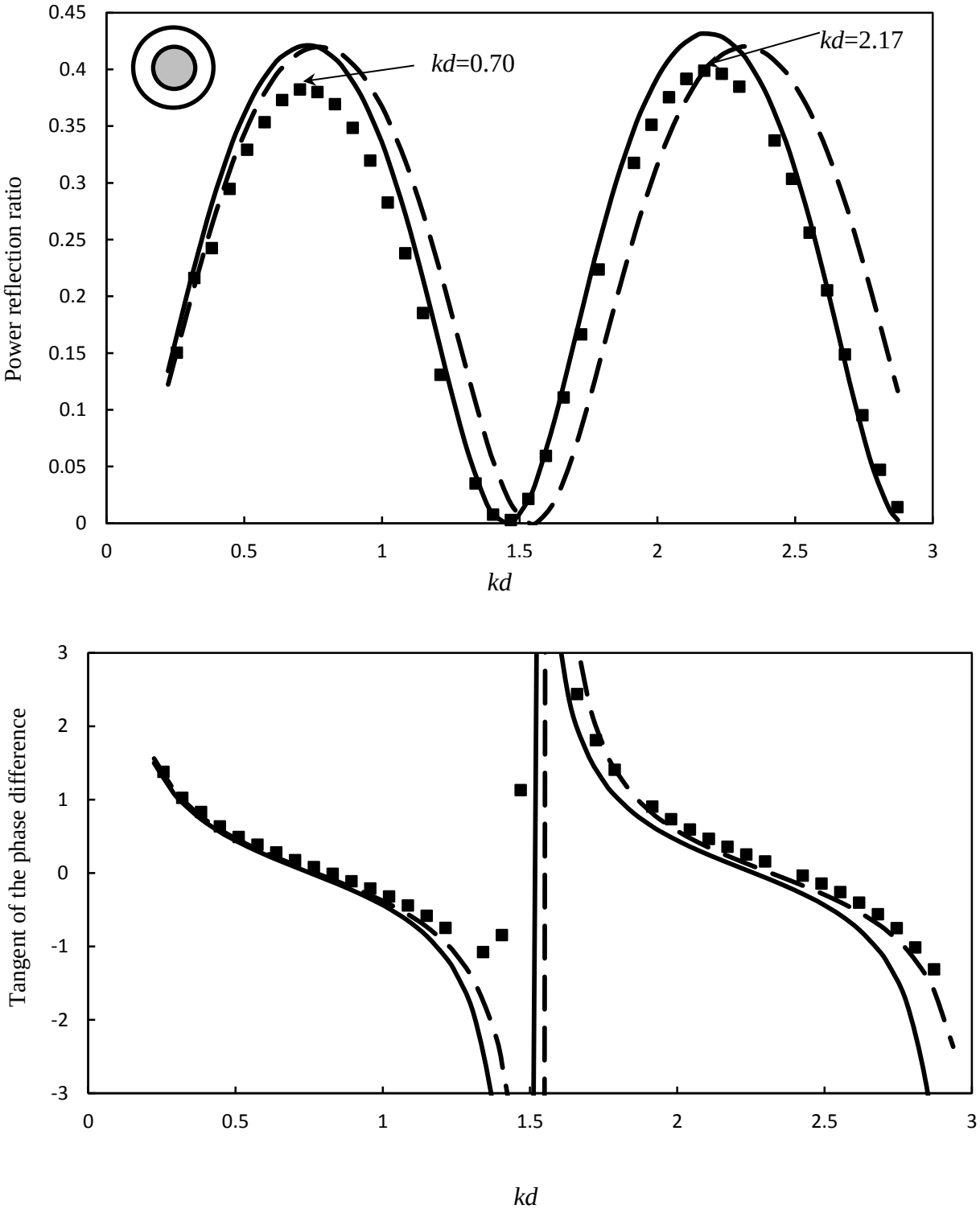

Fig. 2(a) Power reflection ratio Λ , (b) tangent of the phase difference ψ: ——, FE model; ─ ─ , plane wave model; ■ ■ ■ , experiment.

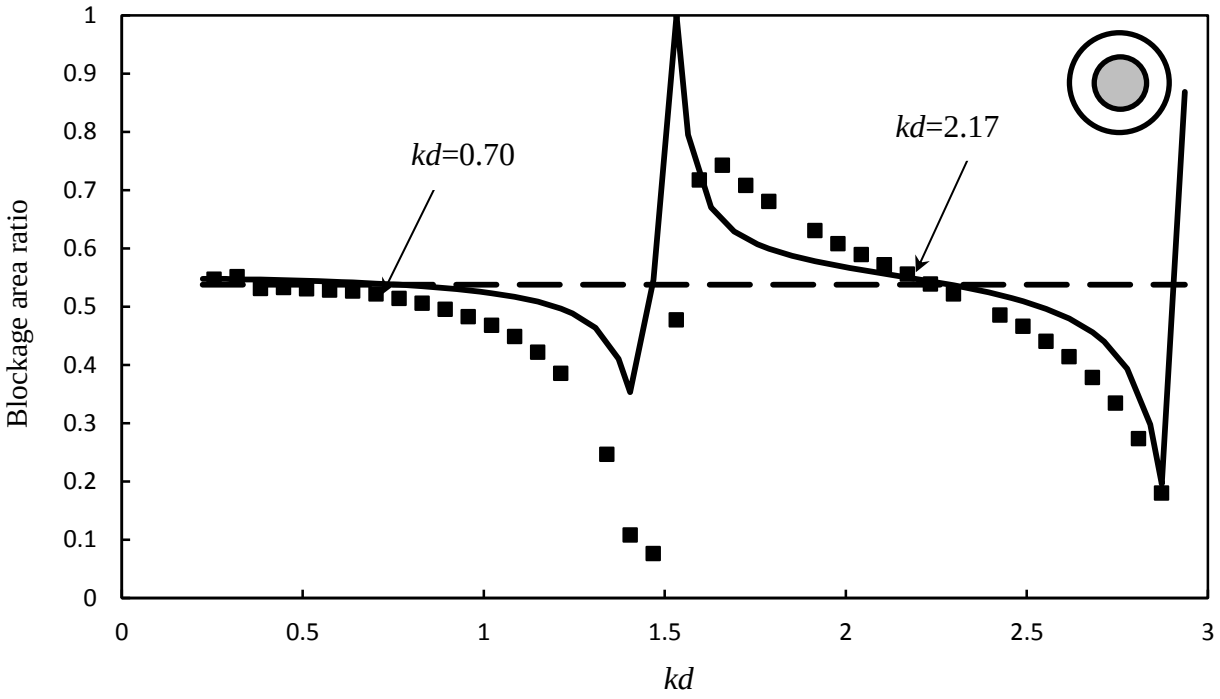

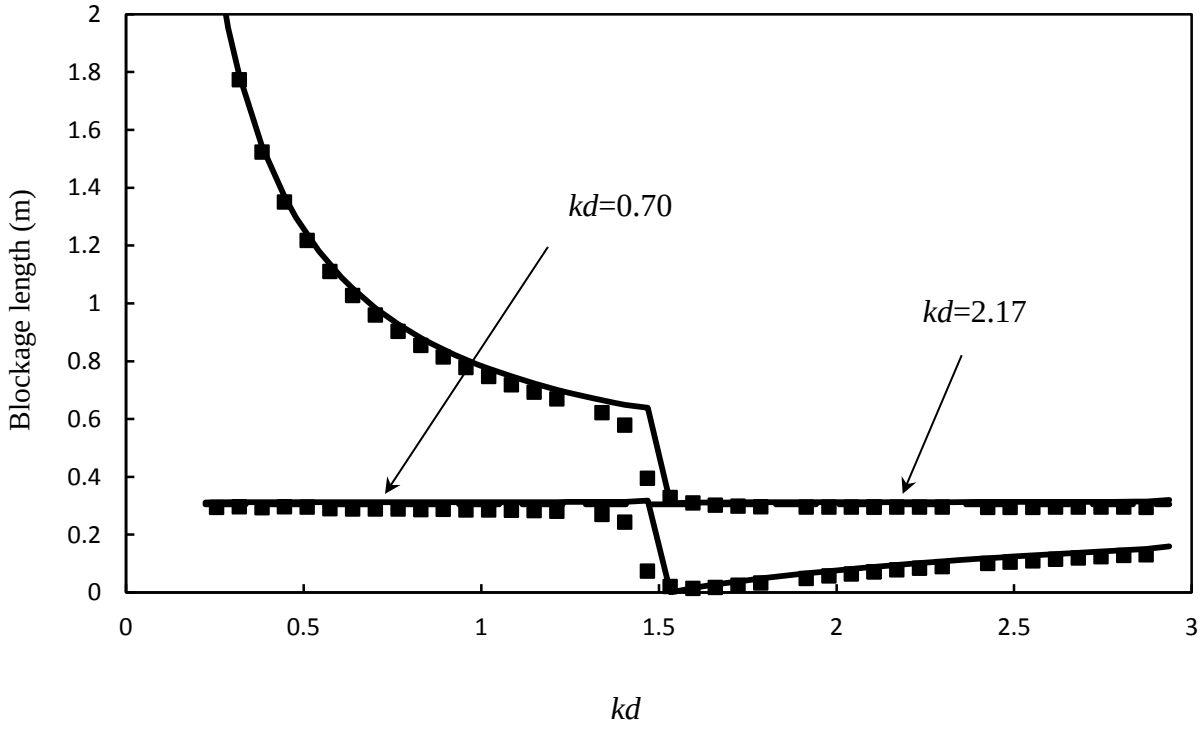

Fig. 3(a) Blockage area ratio, (b) blockage length: ——, FE model; ■ ■ ■ , experiment; ─ ─ ─ , actual blockage size.

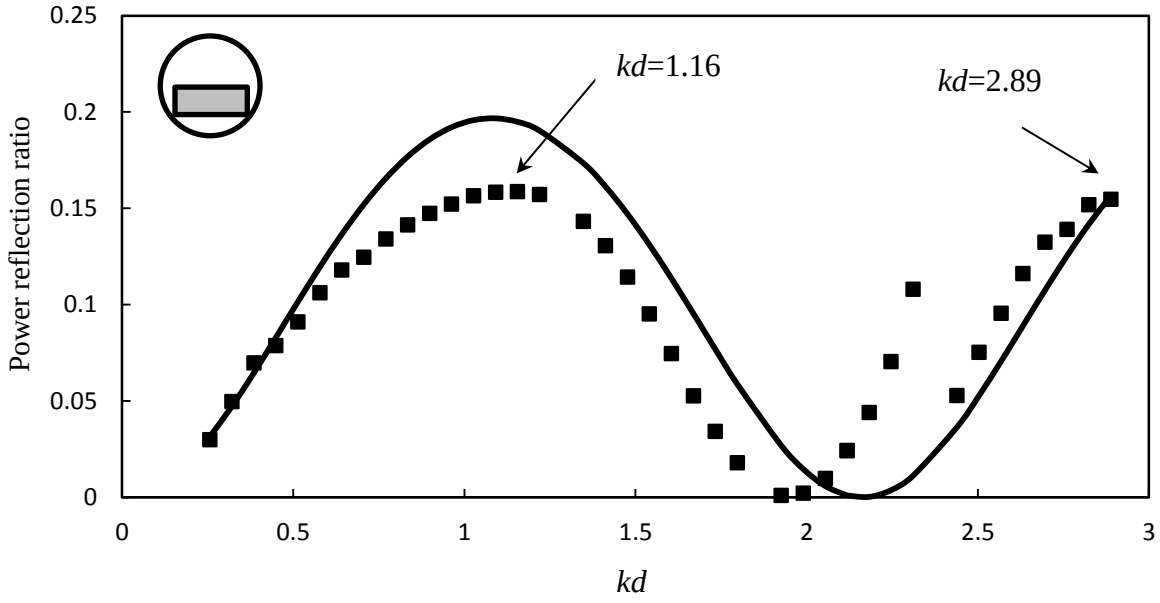
0.25
0.2
0.15
0.1
0.05
0
Power reflection ratio
kd=1.16
kd=2.89
0
0.5
1
1.5
2
2.5
3
kd

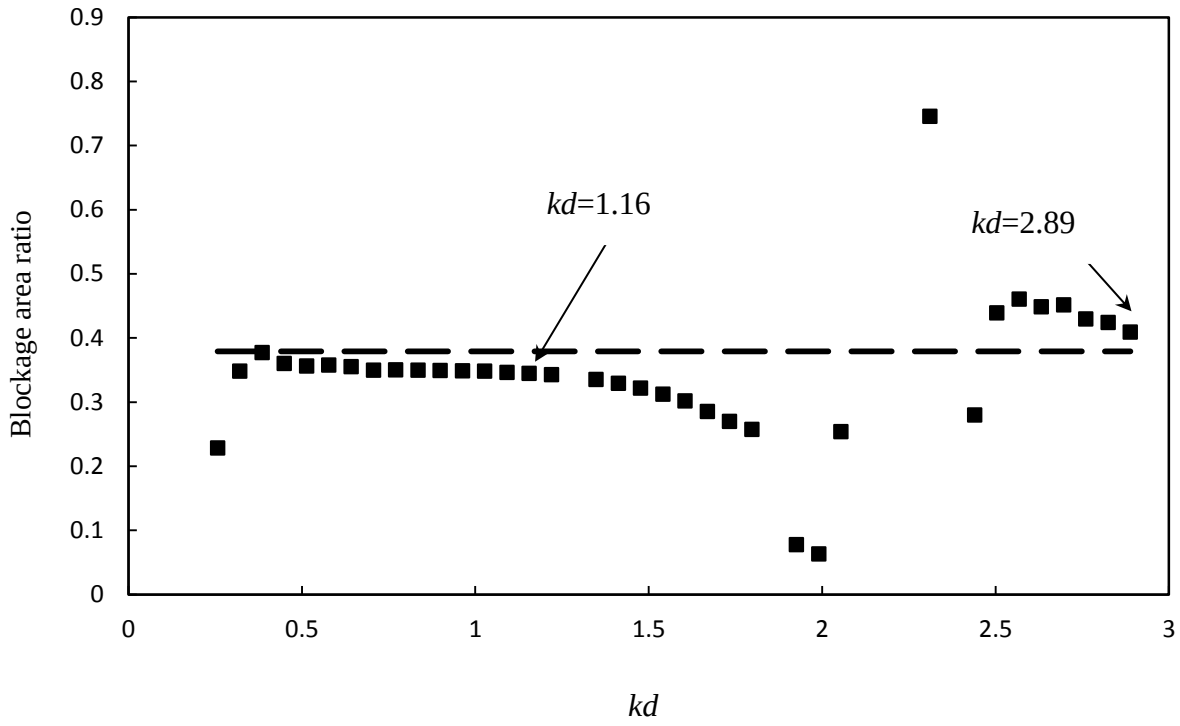
0.9
0.8
0.7
0.6
0.5
0.4
0.3
0.2
0.1
0
Blockage area ratio
kd=1.16
kd=2.89
0
0.5
1
1.5
2
2.5
3
kd

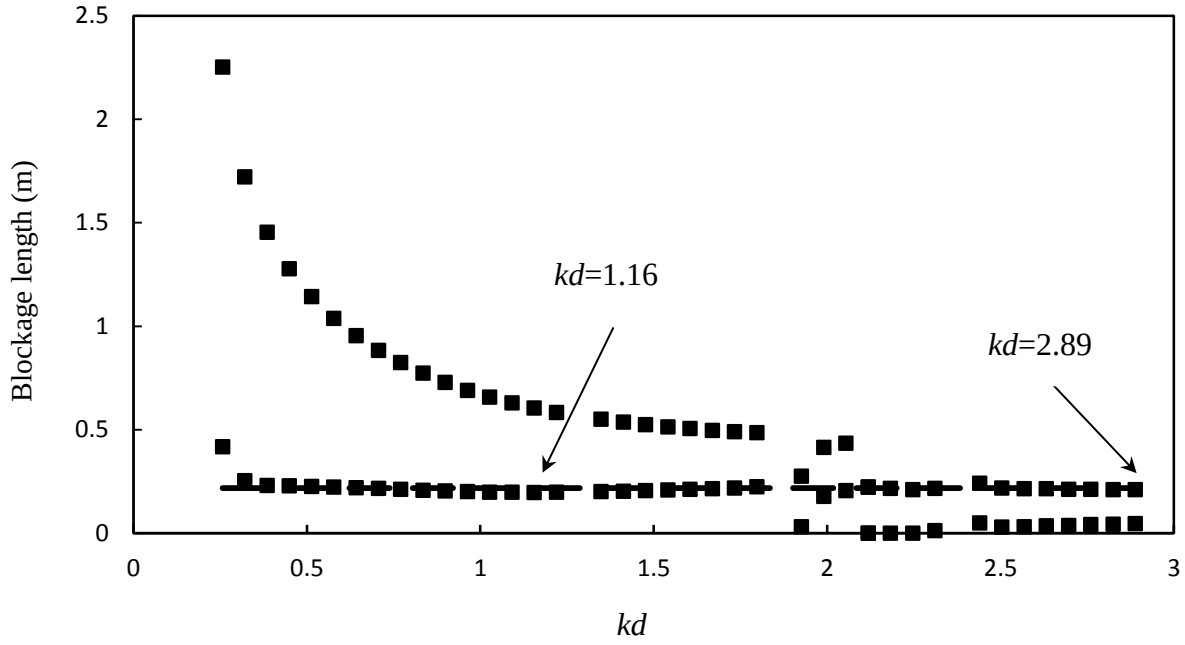

Fig. 4(a) Power reflection ratio Λ , (b) blockage area ratio , (c) blockage length: ——, plane wave model; ■ ■ ■ , experiment; — — — , actual blockage size.

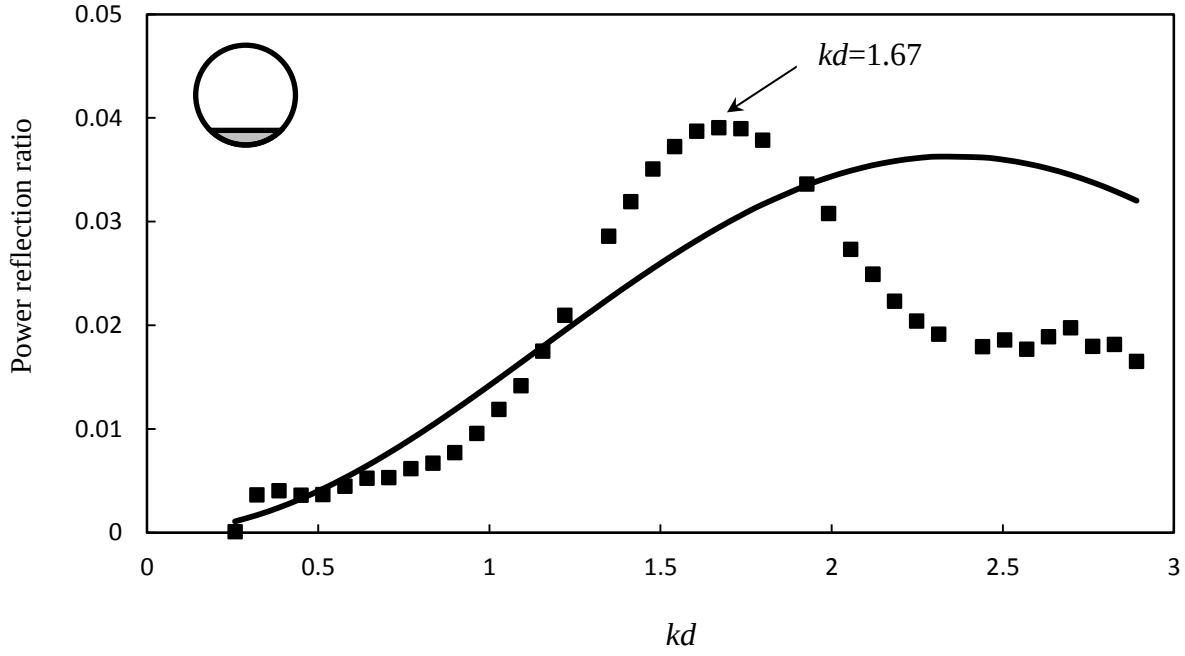

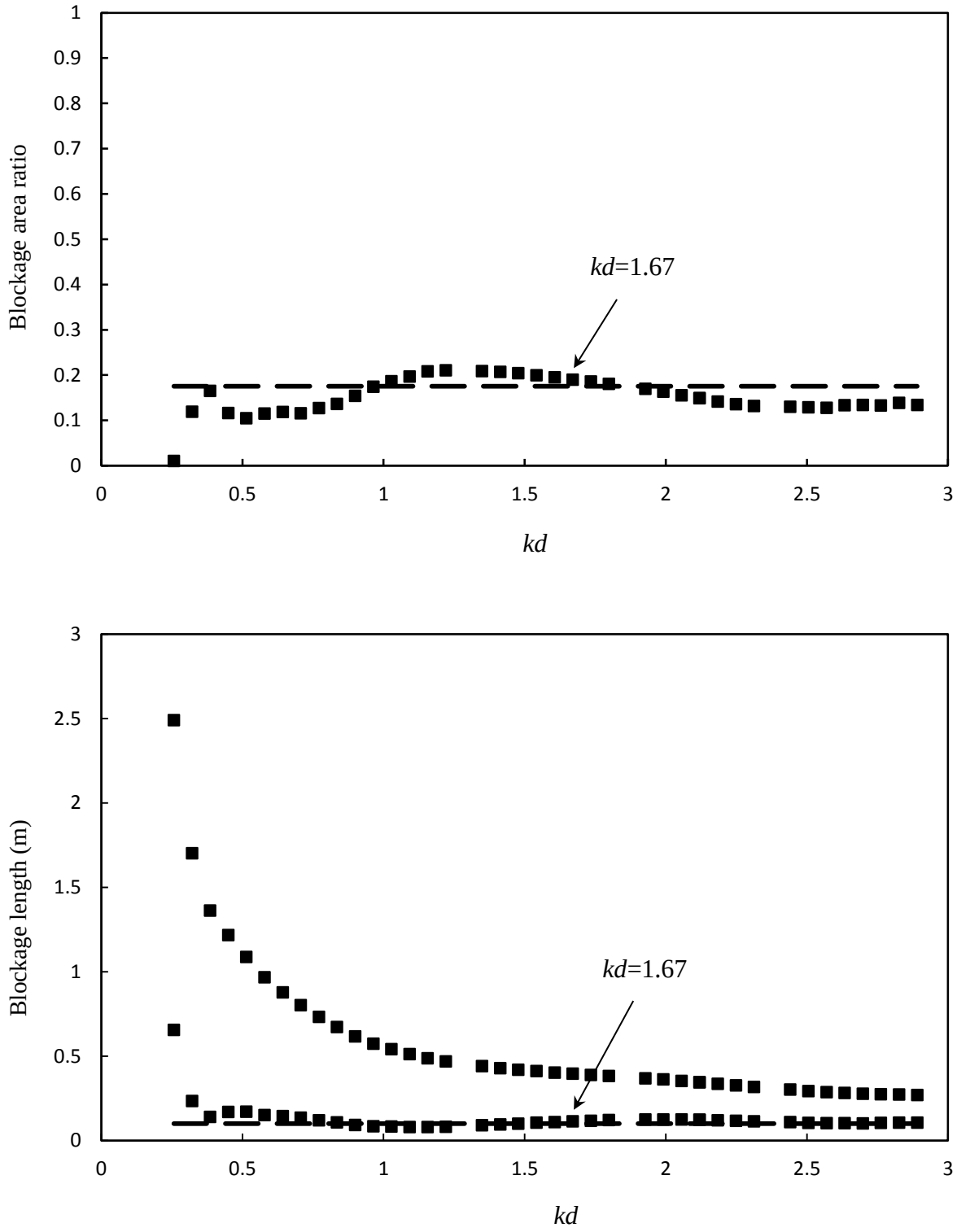

Fig. 5(a) Power reflection ratio Λ , (b) blockage area ratio, (c) blockage length: ——, plane wave model; ■ ■ ■ , experiment; — — — , actual blockage size.

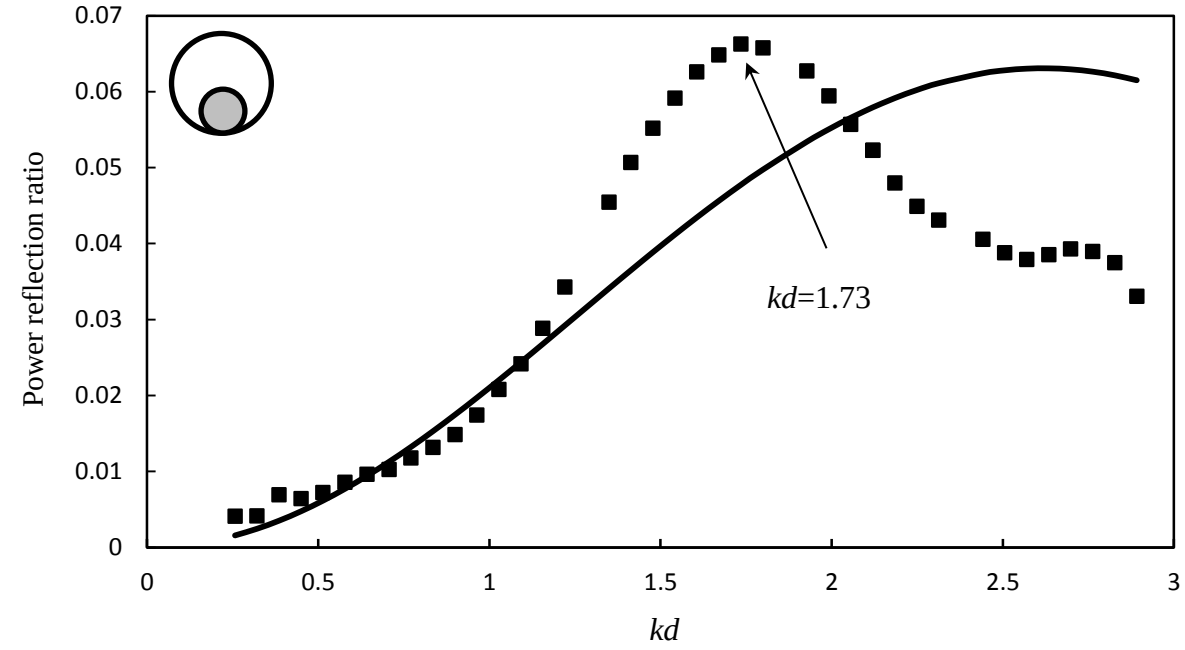
Power reflection ratio
0.07
0.06
0.05
0.04
0.03
0.02
0.01
0
0
0.5
1
1.5
2
2.5
3
kd
kd=1.73

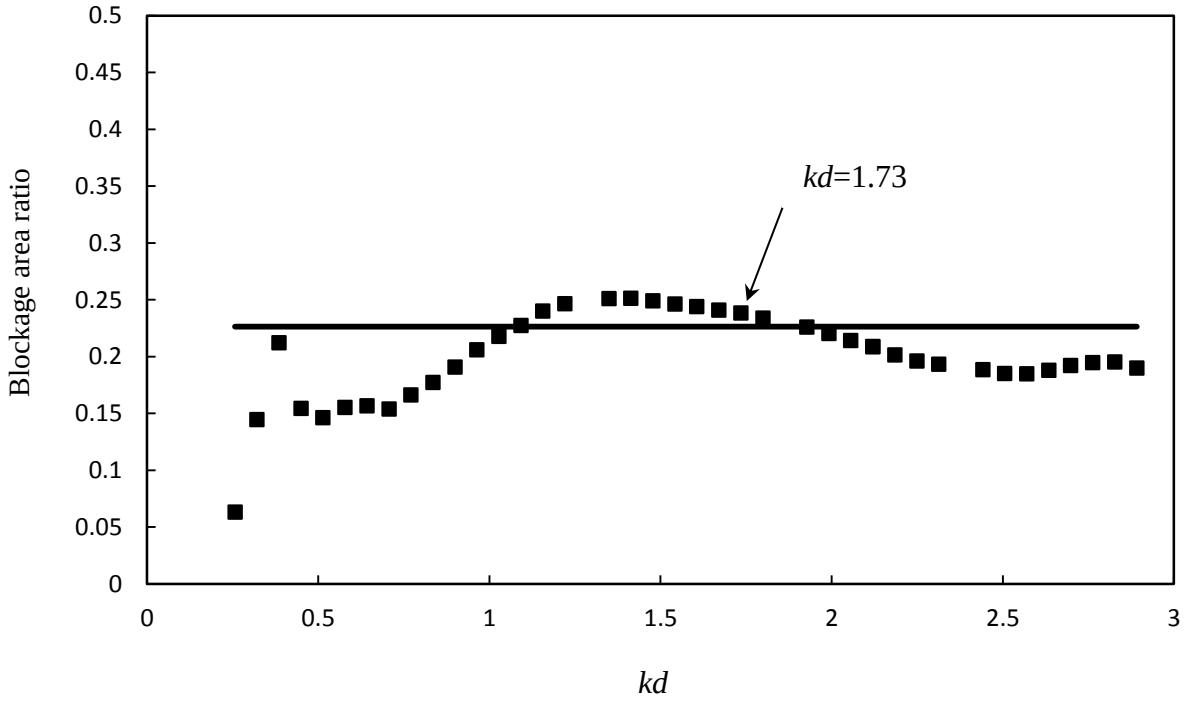
Blockage area ratio
0.5
0.45
0.4
0.35
0.3
0.25
0.2
0.15
0.1
0.05
0
0
0.5
1
1.5
2
2.5
3
kd
kd=1.73

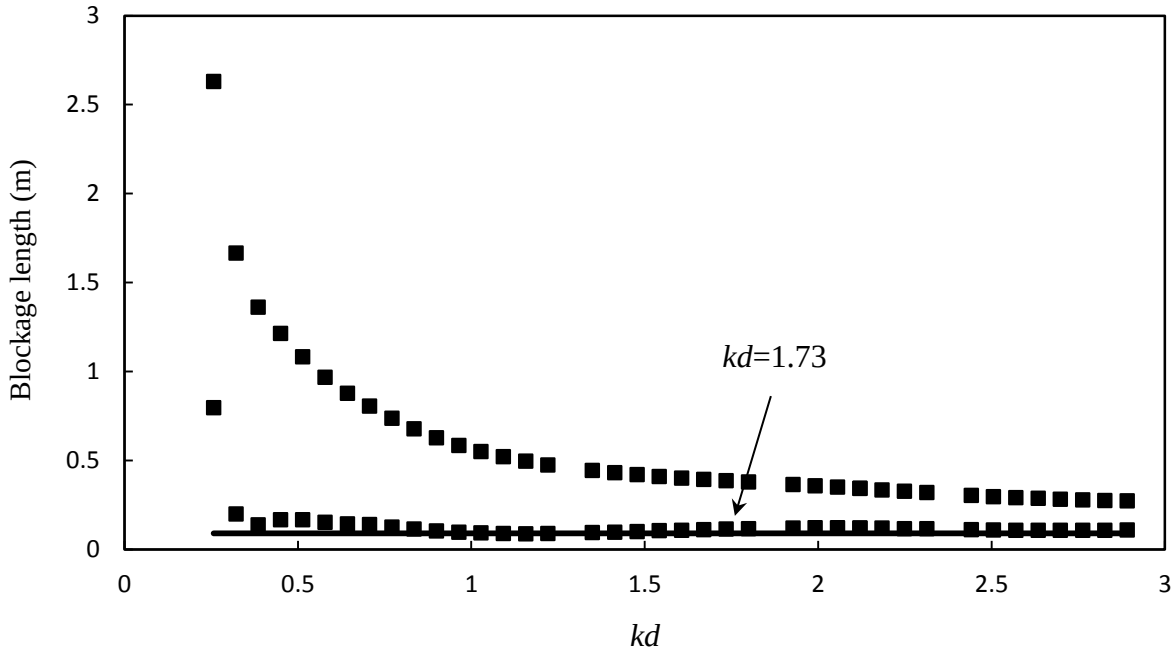

Fig. 6(a) Power reflection ratio Λ , (b) blockage area ratio, (c) blockage length: ——, plane wave model; ■ ■ ■ , experiment; — — — , actual blockage size.

Table 1. Experiments with various blockages

No.	Shape	Dimensions (m)	Area ratio			Length L_b (m)		
			Actual	Predicted	Error (%)	Actual	Predicted	Error (%)
1	Brick	W0.105× H0.032× L_b0.214	0.192	0.215	12.0	0.214	0.197	7.9
2	Brick	W0.104× H0.018× L_b0.216	0.108	0.115	6.5	0.216	0.201	6.9
3	Brick	W0.075× H0.065× L_b0.072	0.277	0.282	1.8	0.072	0.087	20.8
4	Brick	W0.063× H0.049× L_b0.103	0.175	0.186	6.3	0.103	0.120	16.5
5	Brick	W0.103× H0.049× L_b0.063	0.283	0.284	0.4	0.063	0.084	33.3
6	Cylinder	R0.017× L_b0.147	0.051	0.087	70.6	0.147	0.162	10.2
7	Half moon	R0.15× H0.065× L_b0.08	0.413	0.560	35.6	0.08	0.071	11.3
8	Trapezoid prism	R0.15× W0.15× H0.065× L_b0.078	0.362	0.406	12.2	0.078	0.080	2.6
9	Wooden block	W0.058× H0.047× L_b0.215	0.153	0.162	5.9	0.215	0.226	5.1
10	Wooden block	W0.09× H0.09× L_b0.045	0.458	0.437	4.6	0.045	0.062	37.8

(a) Brick or wooden block

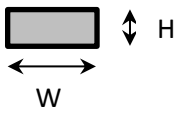

(b) Cylinder

(c) Half moon

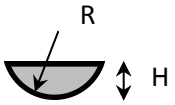

(d) Trapezoid prism

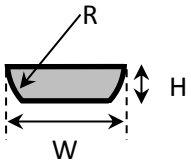

Fig. 7 General shapes of the blockages used in Table. 1.